FARMACIA, 2025, Vol. 73, 6

https://doi.org/10.31925/farmacia.2025.6.5 **ORIGINAL ARTICLE**

EXPLORING NOVEL PATHWAYS MODULATED BY PIOGLITAZONE THROUGH NETWORK PHARMACOLOGY AND GENE EXPRESSION ANALYSIS

DALILA BALDERAS-RENTERIA [1], BRYAN ALEJANDRO ESPINOSA-RODRIGUEZ [2], KARLA RAMIREZ-ESTRADA [2], NANCY ELENA GUZMAN-DELGADO [4], XRISTO ZARATE [3], KATIUSHKA AREVALO-NIÑO [1], ISAIAS BALDERAS-RENTERIA [2]*

[1]*Universidad Autonoma de Nuevo Leon, Facultad de Ciencias Biologicas, Instituto de Biotecnologia, San Nicolas de los Garza, Nuevo Leon, 66455, Mexico*
[2]*Universidad Autonoma de Nuevo Leon, Facultad de Ciencias Quimicas, Laboratory of Molecular Pharmacology and Biological Models, Monterrey, Nuevo Leon, 64570, Mexico*
[3]*Universidad Autonoma de Nuevo Leon, Facultad de Ciencias Quimicas, Laboratory of Protein Expression and Purification, Monterrey, Nuevo Leon, 64570, Mexico*
[4]*Health Research Division, High Specialty Medical Unit, Cardiology Hospital N. 34. Mexican Social Security Institute, Monterrey 64360, Mexico*

**corresponding author: isaias.balderasrn@uanl.edu.mx*

Manuscript received: August 2025

Abstract

Type 2 diabetes mellitus (T2DM) is a metabolic disorder characterised by chronic hyperglycaemia and insulin resistance (IR), leading to severe complications. Pioglitazone, a PPARγ agonist, improves glycaemic control but is limited by adverse effects, such as weight gain, oedema and risk of fractures. This study aimed to investigate the molecular actions of pioglitazone to identify novel therapeutic targets for safer and more selective treatments. Using network pharmacology, 100 targets were predicted for pioglitazone, including PPARγ, mTOR and GSK-3β. Comparative analyses identified 49 and 90 overlapping targets with T2DM and IR, respectively. Enrichment analyses highlighted key pathways, including PI3K-Akt, FoxO and AGE-RAGE signalling, as well as carbohydrate metabolism and endoplasmic reticulum (ER) stress. Experimental validation in a diabetic murine model confirmed these findings, revealing significant transcriptomic modulation in the liver. Pioglitazone upregulated genes were involved in glucose homeostasis and cellular stress responses, while downregulated genes were involved in oxidative stress and inflammation pathways. Notably, pioglitazone exerted broader effects than recombinant PPARγ, suggesting PPARγ-independent actions. Novel targets, such as ketohexokinase and ER stress components, were identified as promising candidates for future therapies. This integrative approach highlights the potential of combining computational and experimental strategies for drug discovery in T2DM.

Rezumat

Acest studiu a avut ca scop investigarea acțiunilor moleculare ale pioglitazonei pentru identificarea unor noi ținte terapeutice care să permită dezvoltarea unor tratamente mai sigure și mai selective. Prin farmacologia de rețea, au fost găsite 100 de ținte pentru pioglitazonă, PPARγ, mTOR și GSK-3β. Analizele comparative au identificat 49, respectiv, 90 de ținte comune cu T2DM și IR. Analizele de îmbogățire au evidențiat căi importante, precum semnalizarea PI3K-Akt, FoxO și AGE-RAGE, precum și procese legate de metabolismul glucidic și stresul reticulului endoplasmatic (ER). Aceste rezultate au fost validate experimental într-un un model murin de diabet zaharat de tip 2, revelând o modulare transcriptomică semnificativă la nivel hepatic. Genele supraexprimate sub acțiunea pioglitazonei au fost implicate în homeostazia glucozei și răspunsul la stresul celular, în timp ce genele subexprimate aparțineau căilor de stres oxidativ și inflamație. Pioglitazona a exercitat efecte mai ample decât PPARγ recombinant, sugerând acțiuni independente de PPARγ. Noi ținte, precum cetohexokinaza și componente ale stresului ER, ar putea deveni candidați promițători pentru terapiile viitoare.

Keywords: PPARγ, type 2 diabetes mellitus, network pharmacology, pioglitazone

Introduction

According to the American Diabetes Association, T2DM is an endocrine-metabolic disease characterised by persistent episodes of hyperglycaemia due to impaired glucose utilisation by peripheral tissues and increased gluconeogenesis or glycogenolysis resulting from IR [1]. The failure to control glycemia in T2DM is associated with the appearance of macrovascular complications, including myocardial infarction, stroke and peripheral vascular disease (diabetic foot), and with the development of microvascular complications, including neuropathy, retinopathy and nephropathy [2]. Pharmacological treatments are an essential component of the holistic management of T2DM

and have been proven to prevent the development of complications [3].

Thiazolidinediones, also known as glitazones, are insulin-sensitising medications used to manage T2DM. Their biological actions are mediated by binding and activating the peroxisome proliferator-activated receptor γ (PPARγ). This receptor is a ligand-dependent transcription factor that belongs to the nuclear hormone receptor superfamily and is activated by endogenous ligands, such as the unsaturated fatty acids and the eicosanoids, as well as by synthetic thiazolidinediones, including rosiglitazone, troglitazone and pioglitazone [4].

In its basal state, PPARγ binds to its partner retinoid X receptor α (RXRα) at peroxisome proliferator-activated receptor response elements (PPREs), a hexameric sequence (AGGTCANAGGTCA) located in the promoter and enhancer regions of PPARγ target genes. Additionally, the transcriptional activity of PPARγ is blocked by the presence of corepressors NCoR and SMRT that recruit histone deacetylase complexes to promote chromatin condensation and reduce gene expression. Once activated, PPARγ undergoes a conformational change that releases corepressors and promotes the binding of coactivators, such as P300 and SRC1, which recruit histone-remodelling machinery to promote the chromatin de-condensation, leading to the up- or down-regulation of PPARγ target genes [4, 5].

Some biological actions attributed to PPARγ activation include the differentiation of preadipocytes into mature adipocytes through the upregulation of genes implicated in the uptake and metabolism of lipids, including *CD36*, *LPL*, *FABP4*, among others [5, 6]; the browning of subcutaneous white adipocytes into beige adipocytes by promoting the stabilisation of the protein levels of PRDM16, that is the master transcriptional regulator of brown adipocytes [7]; the insulin sensitisation in peripheral organs through the modulation of the visceral adipose tissue biology that leads to decreased circulating free fatty acids, contributors of the so-called lipotoxicity, and increased circulating adiponectin [8, 9]; the glucose-stimulated insulin secretion from pancreatic β-cells *via* upregulation of GPR-40 and GLUT2, and an increased calcium mobilisation [10]; and some immunomodulatory effects that lower inflammation [11]; all these effects contribute to reverse IR [12]. However, given PPARγ's pleiotropic expression across several tissues, its activation is associated not only with its desired antidiabetic effects but also with undesired adverse effects. For instance, treatment with thiazolidinediones can diminish osteoblastogenesis and increase osteoclastogenesis [12]. Indeed, pioglitazone was reported to increase the risk of fractures in treated patients compared to placebo and to improve the markers of bone resorption [13, 14]. Additionally, thiazolidinediones, especially pioglitazone, have been associated with weight gain, volume retention and oedema, and with exacerbation of severe heart failure [15-18]. For this reason, according to the American Diabetes Association, despite their high efficacy as antidiabetic drugs, thiazolidinediones are not considered first-line treatments for the management of T2DM [19].

The biology of PPARγ is far from being elucidated, as new information and advances about effector pathways, functions, regulation, or applications in other diseases are constantly being published. In the case of T2DM, the main PPARγ agonists, *i.e.*, thiazolidinediones, are being displaced by safer options, such as glucagon-like peptide-1 receptor agonists and sodium-glucose cotransporter 2 inhibitors, that offer high antidiabetic efficacy, cardiovascular and renal protective effects and mild adverse effects. However, in recent years, new lines of research have been conducted to surpass some limitations associated with the full agonism of PPARγ, including the development of partial agonists. Similarly, the study of the molecular actions of pioglitazone may allow the identification of pathways and new therapeutic targets that could be druggable and relevant for the treatment of T2DM, while overcoming the limitations of current thiazolidinediones.

For these reasons, in the present study, we employed a network pharmacology approach to identify potential pathways or targets modulated by pioglitazone. These findings were validated using differentially expressed genes from a diabetic murine model treated with the drug, as analysed by DNA microarray.

Materials and Methods

Structure-dependent target prediction for pioglitazone

We retrieved the isomeric SMILES of pioglitazone from PubChem. Then, we accessed the SwissTarget Prediction tool (http://www.swisstargetprediction.ch/) and introduced the isomeric SMILES of pioglitazone [20]. After this, we collected the predicted targets in a .CSV file that included the predicted target name, common name, Uniprot ID, ChEMBL ID, target class, probability and known actives (2D/3D).

Collection of genes involved in T2DM and IR

We accessed the GeneCards database (https://www.genecards.org/) and searched for the terms “Type 2 diabetes mellitus” and “Insulin resistance” to retrieve genes associated with these processes [21]. These genes were collected in a .CSV file that contained gene symbols, descriptions, categories, UniProt IDs and relevance scores.

Comparison between the targets of pioglitazone and the collected genes

We accessed the Bioinformatics & Evolutionary Genomics webpage (https://bioinformatics.psb.ugent.be/webtools/Venn/) to generate Venn diagrams comparing the predicted targets for pioglitazone with genes involved in T2DM and IR. The common genes were collected for further analysis.

Identification of pathways or targets modulated by pioglitazone

The common genes identified in the last step were uploaded to STRING (https://string-db.org/) to generate a protein-protein interaction network for the predicted pioglitazone targets. This network was sent to the Cytoscape to identify the top 20 hub genes [22]. Then, these genes were introduced into ShinyGO 0.81 to identify the enriched pathways in which the pioglitazone-associated targets are involved [23].

General animal management

All mice were weighed weekly on an analytical balance from birth until the day of sacrifice to monitor their weight throughout the study. The growth conditions were maintained as specified by the Mexican regulation NOM-062-ZOO-1999. The C57BL/6 mice were kept in cages with water and food *ad libitum*, light and dark cycles of 12 h each, and an environmental temperature between 22°C and 25°C. In this study, a total of 35 male mice were selected for both the standardisation of the diabetic murine model and the assessment of treatments over the diabetic murine model. Before these experiments, mice of the same age and weight were selected and randomly assigned to the different groups. Randomisation consisted of assigning numbers to each mouse; the groups were then created using an online random-number generator (random.org). Notably, there was no blinding during the experiments and data analysis. The intraperitoneal administration of drugs began with immobilisation of the head and neck, maintaining the vertebral column straight by stretching the legs and tail. In this position, the intraperitoneal area was clear, and the injection was performed in the abdominal area, with the other hand. The intravenous infusion was performed using an immobilisation device that allows easy manipulation of the tail. The mice were introduced there, and the injection was administered into the caudal tail vein. The blood samples for glucose and triglyceride determinations were collected by cutting the distal end of the tail, while liver samples destined for transcriptomics were obtained from animals previously anaesthetized, euthanised by decapitation, as stated by the Mexican regulation in NOM-062-ZOO-1999, and collected by dissection.

Generation of the diabetic murine model

The first step in our methodology was identifying the optimal conditions for inducing hyperglycaemia in C57BL/6 mice. For this reason, we performed an experimental design in which four groups of mice (each with n = 5) were exposed to (1) a standard diet composed of carbohydrates (61.66%), protein (20%), fat (9.81%), ashes (6.38%) and fibre (2.15%); (2) a standard diet supplemented with fructose (FRUC), composed of the regular diet and a solution of both fructose 15% and dextrose 1% instead of water; (3) a high-fat diet (HFD), composed of the regular diet (60%) and pork fat (40%); and (4) a high-fat diet supplemented with fructose (HFD + FRUC). These dietary regimens lasted 90 days (approximately 12 weeks), but half of the mice were injected with a single dose of streptozocin (100 mg/kg). The sample size was determined considering a significance level (α) of 0.05, a statistical power (1 - β) of 80%, a standard deviation of 50 mg/dL and a minimum expected effect size of 80 mg/dL for glycemia induced by diets. Inclusion criteria for mice included an age of 4 weeks, male sex, maintenance under controlled laboratory conditions, an initial body weight between 9 g and 14 g, and absence of clinical signs of disease, such as infections or tumours. Exclusion criteria included insufficient response to diabetization, evidence of stress or severe illness, intolerance to any of the treatments, abnormal behaviour, or accidental exposure to uncontrolled environmental conditions. These inclusion and exclusion criteria were established *a priori*. We assessed the weight and the serum glucose levels on days 0, 45 and 90 for each mouse.

Design and implementation of the study groups

To study the effects of recombinant PPARγ or pioglitazone in a diabetic murine model, the experimental design included three groups of mice (n = 5 *per* group). The sample size was determined based on a significance level (α) of 0.05, a statistical power (1 - β) of 80%, a standard deviation of 50 mg/dL and a minimum expected effect size of 80 mg/dL for glycemia reduction induced by the treatments. Mice were subject to the same inclusion and exclusion criteria mentioned in the past section.

The diabetic (DB) group included mice fed *ad libitum* a high-fat diet supplemented with fructose, as previously mentioned. This regimen lasted 12 weeks, but at half mice were injected with a single dose of streptozocin (100 mg/kg). The group of diabetic mice treated with recombinant PPARγ (DB + PPAR) recapitulates the same conditions as DB, but they were treated with 30 µg/kg of recombinant PPARγ on days 79 and 86, *i.e.*, with a week between administrations. Finally, the group of the diabetic mice treated with pioglitazone (DB + PIO) recapitulated the same conditions as DB, but they received 14 mg/kg pioglitazone on days 79 and 86. By the end of the exposition, each mouse was sedated with a mixture of ketamine and xylazine, and once the animal was deeply anaesthetized, it was decapitated, and blood was collected. After that, the body was dissected to extract the liver. It is noteworthy that two mice from each group were excluded from the experiments according to the exclusion criteria we established.

In this study, the primary objective was to investigate the differential effects of recombinant PPARγ and pioglitazone in a diabetic murine model. Given the well-documented metabolic alterations in non-diabetic control mice compared to diabetic counterparts, including a control group, it was deemed unnecessary for this experimental design. The focus of the investigation

was not on establishing baseline differences between healthy and diabetic states, which have been extensively characterised in previous research, but rather on discerning the specific molecular and physiological effects of the therapeutic interventions (recombinant PPARγ and pioglitazone) within a diabetic context. Moreover, including a control group would have required additional animals, which was avoided to adhere to the principles of the 3Rs (Replacement, Reduction and Refinement) in animal research. By limiting the number of groups and focusing solely on the diabetic state, the study was designed to maximise the statistical power of comparisons between treated and untreated diabetic groups while minimising the unnecessary animal use.

Drug preparation and administration

Streptozocin was administered *via* intraperitoneal injection. STZ was freshly prepared before each injection in 0.1 M sodium citrate buffer (pH 4.5), protected from light and administered within 10 minutes of dissolution. Pioglitazone was administered intraperitoneally at a dose of 14 mg/kg. The compound was dissolved in a freshly prepared sterile DMSO/ PBS solution before each injection. Recombinant PPARγ was administered *via* tail vein injection at a dose of 30 μg/kg in sterile saline solution (NaCl 0.9%). Injections were performed using 30 G insulin syringes to a final volume of 5 mL/kg. Mice were warmed under a heat lamp before the injection to dilate the tail veins and minimise stress. Solutions were endotoxin-free and freshly prepared.

Production and purification of the recombinant PPARγ

The complete production and purification of the recombinant PPARγ, including the design of vectors, digestions and ligations, transformation of bacteria, identification and selection of transformed bacteria, and induction of expression and purification, were performed as previously reported by our research group [24].

Determination of serum glucose in the study

After collecting the blood samples, these were incubated at room temperature until clot formation. Then, the samples were centrifuged at 2000 rpm for 10 minutes, and after this, the serum was isolated. The glucose concentration was determined using the glucose oxidase method. The reagents were acquired from Randox, and the methodology was followed according to the instructions of the manufacturer.

Determination of serum triglycerides in the study

After collecting the blood samples, these were incubated at room temperature until clot formation. Then, the samples were centrifuged at 2000 rpm for 10 minutes, and after this, the serum was isolated. The triglyceride concentration was determined using the GPO-PAP method. The reagents were acquired from Randox, and the methodology was followed according to the instructions of the manufacturer.

Determination of the impact of recombinant PPARγ or pioglitazone on the transcriptome of liver cells from diabetic mice

The total RNA was extracted from the isolated liver tissues employing the TRIzol methodology. The total RNA was retrotranscribed and labelled to obtain the corresponding amminoallyl-cDNAs. This step was performed using the commercial Chipshot kit from Promega. The amminoallyl-cDNAs from the DB group were conjugated to AlexaFluor 555, while the DB + PPAR and DB + PIO groups were conjugated to AlexaFluor 647. The conjugation reaction began with the dissolution of aminoallyl-cDNAs in 5 μL of nuclease-free water, and the solution was heated in a water bath at 42°C for 5 minutes. After this, 3 μL of reaction buffer was added to the solution of amminoallyl-cDNAs. Then, 8 μL of this new solution was mixed with a solution of AlexaFluor 555 or AlexaFluor 647, depending on the specific group from which RNA was extracted. Finally, 72 μL of water was added to this solution. To perform the hybridisation with the microarray, 25 μL of one sample labelled with AlexaFluor 555 and one sample labelled with AlexaFluor 647 were dried in DyNAvap. Both samples were resuspended with 7 μL of water, and 10 μL of SSC 20X, 4 μL of SDS 0.1%, and 12 μL of TE 1X were added. The samples were denatured at 94°C for 5 minutes and at 65°C for 30 seconds. Then, the samples were transferred onto the microarray surface, a coverslip was applied, and the chip was incubated at 42°C for 12 - 18 hours. After incubation, the chip was washed three times with 50 mL of SSC 1X-SDS 0.5% for 2 minutes, and with 50 mL of SSC 0.06X for 2 minutes. The chip was dried by centrifugation and read in a microarray scanner at 555 nm and 647 nm.

Bioinformatic analysis of transcriptomic data

Using DNA microarray data, genes with Z-scores greater than 2 (upregulated) or less than -2 (down-regulated) in either the PIO or PPARγ treatment were compared with genes associated with T2DM or IR. Common genes across conditions were collected and submitted to the ShinyGO 0.81 tool for functional annotation. The FDR cutoff employed was 0.05; the minimum and maximum pathway size were 2 and 5000; and the option to remove redundancy was activated. The enriched pathways were collected for their analysis and discussion.

Statistical analysis

Before the statistical analysis, the normality of the collected data was assessed using the Shapiro-Wilk test. The data collected on weight gain and serum glucose during standardisation of the diabetic murine model were analysed using the Kruskal-Wallis test and the Dunn's post hoc test for multiple comparisons. In the same way, the data collected during biochemical assessments from untreated and treated mouse groups were analysed using two-way ANOVA or one-way ANOVA, depending on the number of variables tested.

For multiple-comparison analysis, we used Tukey's and Sidak's post hoc tests. We used GraphPad Prism 8 (version 8.0.2) to perform the statistical analysis and generate the figures presented here.

Results and Discussion

Structure-dependent target prediction of pioglitazone

After introducing the isomeric SMILES of pioglitazone in the SwissTargetPrediction tool, the platform retrieved 100 predicted targets. Some of these targets were predicted with 94% probability, and, as expected, they included PPARα and PPARγ. Unexpectedly, monoamine oxidase B, carbonic anhydrase II, and the bile salt export pump were also included. With a probability near 10%, some targets included the hexokinase type IV, glycogen synthase kinase 3β, different caspases, cathepsins and receptors. Other predicted targets lacked a probability score but were retrieved because of reported inhibition by structurally related molecules to pioglitazone, including the serine/threonine protein kinase mTOR, protein-tyrosine phosphatase 1B, heat shock protein HSP90 α, different muscarinic receptors, matrix metalloproteinases and tyrosine-protein kinases, among others.

Table I

Structure-dependent target prediction for pioglitazone in the SwissTargetPrediction tool

Target	Common name	Probability score	Known actives (2D/3D)
Monoamine oxidase B	MAOB	0.938790203	10/4
Carbonic anhydrase II	CA2	0.938790203	110/4
Peroxisome proliferator-activated receptor γ	PPARG	0.938790203	683/59
Peroxisome proliferator-activated receptor α	PPARA	0.938790203	369/8
Bile salt export pump	ABCB11	0.938790203	4/3
Thromboxane-A synthase	TBXAS1	0.097239989	107/2
Type-1 angiotensin II receptor (by homology)	AGTR1	0.097239989	222/1
Peroxisome proliferator-activated receptor δ	PPARD	0.097239989	143/2
15-hydroxyprostaglandin dehydrogenase [NAD+]	HPGD	0.097239989	81/5
Free fatty acid receptor 1	FFAR1	0.097239989	81/14
Macrophage colony-stimulating factor receptor	CSF1R	0.097239989	39/0
Vanilloid receptor	TRPV1	0.097239989	158/0
Dihydroorotate dehydrogenase	DHODH	0.097239989	277/0
Epoxide hydratase	EPHX2	0.097239989	130/0
Hexokinase type IV	GCK	0.097239989	43/0
Bombesin receptor subtype-3	BRS3	0.097239989	1/0
Phosphodiesterase 10A (by homology)	PDE10A	0.097239989	209/0
Adenosine A3 receptor	ADORA3	0.097239989	190/2
Cyclin-dependent kinase 9	CDK9	0.097239989	29/0
α-2b adrenergic receptor	ADRA2B	0.097239989	4/1
Epidermal growth factor receptor erbB1	EGFR	0.097239989	187/1
Norepinephrine transporter	SLC6A2	0.097239989	2/1
Glycogen synthase kinase 3β	GSK3B	0.097239989	110/0

Comparison between the predicted targets of pioglitazone against genes involved in T2DM or IR

Once we identified the possible targets underlying pioglitazone's action, we were interested in determining which of these targets are involved in the patho-physiological processes of T2DM or IR. For this reason, we decided to create Venn diagrams comparing the predicted targets with several targets related to these conditions to identify those targets that may explain the anti-diabetic actions of pioglitazone. To do this, first we accessed GeneCards and retrieved genes by searching for the terms "Type 2 diabetes mellitus" or "Insulin resistance". We collected 9,038 and 10,264 genes related to T2DM and IR, respectively. After this, we created the Venn diagrams by comparing the predicted targets of pioglitazone against the genes associated with T2DM or IR, obtaining 49 and 90 common elements, respectively (Figure 1A and Figure 1B). These elements were isolated from the remainder for further analysis.

Identification of possible pathways or targets modulated by pioglitazone according to network pharmacology

After identifying the common elements between the predicted pioglitazone targets and genes associated with T2DM or IR, we introduced these elements into STRING to construct a protein-protein interaction network for each comparison. After this, the networks were sent to Cytoscape to identify the top 20 Hub components. For the comparison between PIO and T2DM, some of the top 20 hub components included PPARG, PPARA, PPARD, MTOR, PTPN1, HSP90AA1 and GSK3B, among others. In the comparison between PIO and IR, some of the top 20 hub components included PPARG, HSP90AA1, GSK3B, MDM2, MET, MAPK14 and MAP2K1, among others. The complete collections of hub components for each comparison are shown in Figure 1C and Figure 1D.

Finally, the top 20 hub components derived from each comparison were introduced into ShinyGO 0.81 to identify the enriched pathways that may be modulated by pioglitazone. The enrichment analysis showed that the hub components associated with T2DM were involved in AGE-RAGE signalling, IR, insulin signalling, lipid and atherosclerosis, apelin signalling, PPAR signalling, T2DM and protein processing in the ER, among others. On the other hand, the enrichment analysis showed that hub components in IR were involved in FoxO signalling, autophagy, PI3K-Akt signalling, IR, insulin signalling, T2DM, diabetic cardiomyopathy and protein processing in the ER. The complete set of pathways for each analysis is shown in Figure 2.

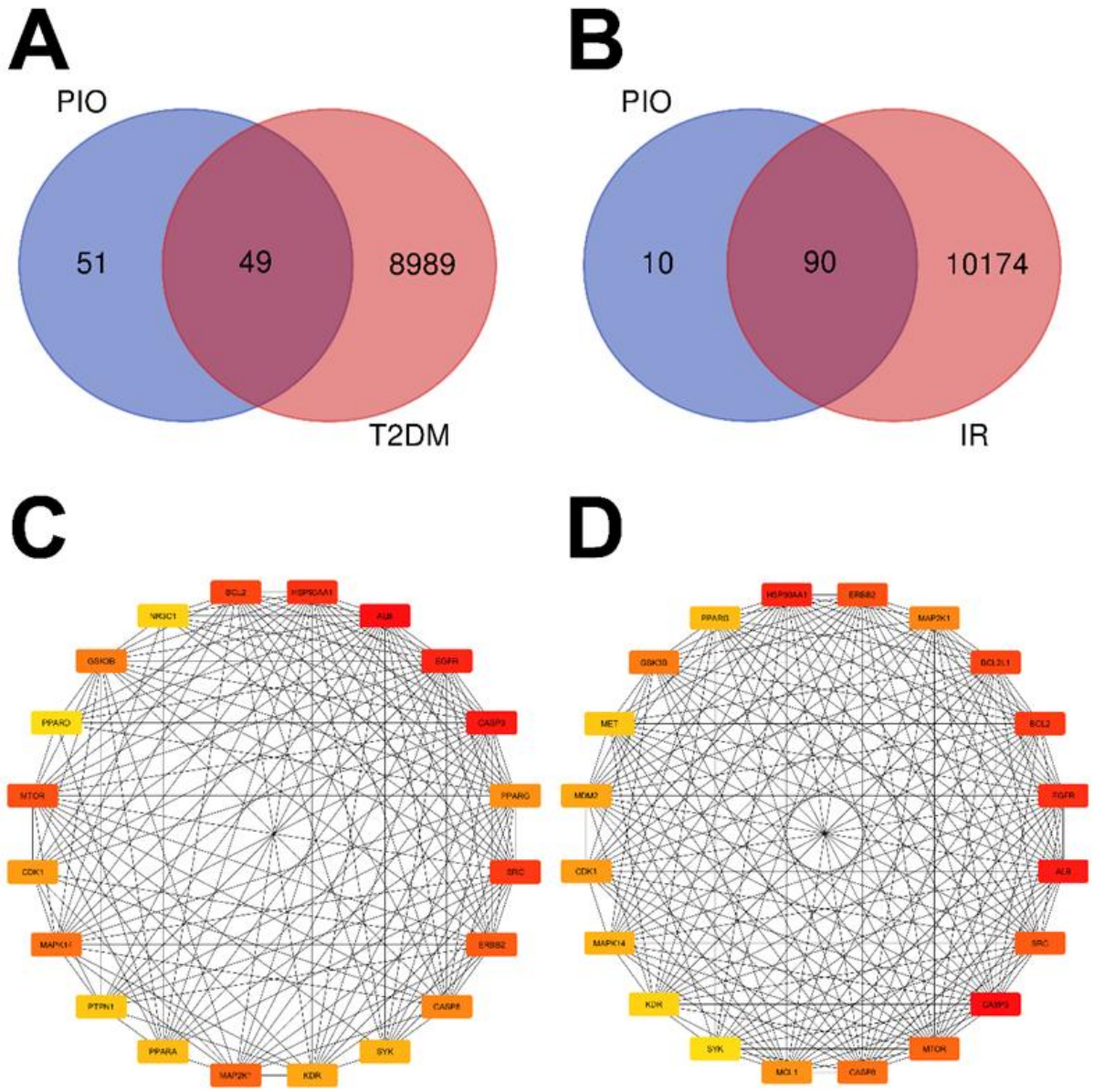

Figure 1.

Comparisons between the predicted targets of pioglitazone and genes associated with T2DM or IR

The Venn diagrams represent the overlap between the predicted molecular targets of pioglitazone and genes linked to T2DM (A) and IR (B). In the IR context, 90 genes overlapped between pioglitazone-predicted targets and those associated with the condition, while 10 genes were exclusive to pioglitazone, and 10,174 were specific to IR-associated genes. For T2DM, 49 genes were shared between pioglitazone targets and T2DM-associated genes, with 51 exclusives to pioglitazone and 8,989 unique to T2DM targets. The network diagrams below were generated in Cytoscape and represent the top 20 hub proteins identified from the common genes in the Venn diagrams above. These hub proteins were ranked by network centrality metrics, indicating their potential importance in the molecular pathways of T2DM (C) and IR (D). The nodes were colour-coded to reflect their significance, with red representing the most critical proteins and yellow indicating lower, but still relevant, importance in the network. This analysis highlights key molecular targets that may mediate pioglitazone's therapeutic effects in these metabolic conditions.

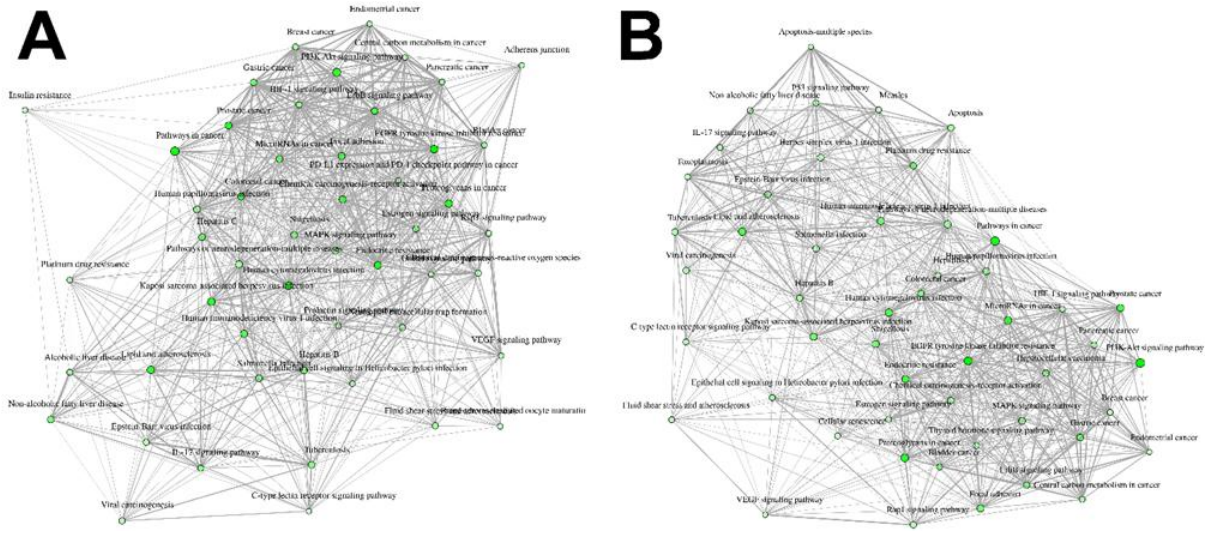

Figure 2.

Enriched pathways affected by the top 20 hub targets of pioglitazone in the context of T2DM or IR

The network diagrams illustrated the enriched pathways derived from the top 20 hub targets identified among the shared genes between the predicted molecular targets of pioglitazone and genes linked to T2DM (A) or IR (B). Each node represents a specific pathway, and edges indicate interactions or shared components between pathways. The green nodes highlight key enriched pathways, emphasising their relevance to T2DM and IR pathophysiology. Pathways such as PI3K-Akt signalling, apoptosis and IR-related mechanisms were prominently featured, reflecting the potential therapeutic impact of pioglitazone through its interaction with these molecular networks.

Establishment of the diabetic murine model

To confirm these theoretical results, we decided to generate a murine model of diabetes through dietary interventions and the exposure to streptozocin and treat these mice with pioglitazone. Then, we analysed the liver transcriptome, one of the major organs affected by the drug, and identified the differentially expressed genes underlying its mechanism of action.

Before inducing diabetes in the mice to be treated, we decided to identify the most effective dietary interventions for inducing hyperglycaemia in C57BL/6 mice. For this proposal, we performed an experimental design in which four groups of mice (each with n = 5) were fed for 12 weeks with (1) a standard diet, (2) a standard diet supplemented with fructose, (3) a high-fat diet, or (4) a high-fat diet supplemented with fructose. Additionally, by the 6th week, the mice were exposed to streptozocin. As shown in Figure 3A, all diets were associated with significant time-dependent increments in weight. In the control group (CT), a substantial increase was observed between day 0 and day 90 ($p < 0.01$). In the FRUC and HFD groups, body weight increased significantly between day 0 and day 45 ($p < 0.01$ for both), with no further significant changes thereafter. In contrast, the HFD + FRUC group exhibited a more sustained gain, with significant increases observed between day 0 and day 45 ($p < 0.01$) and between day 0 and day 90 ($p < 0.05$), suggesting a cumulative effect of the combined dietary components.

In Figure 3B, between-group comparisons showed no significant differences at baseline (day 0). However, by day 45, animals in the FRUC group exhibited significantly lower body weight than both the HFD and HFD + FRUC groups ($p < 0.01$), indicating an early divergence in the weight-gain trajectory. At day 90, the CT group showed significantly higher weight than the FRUC group ($p < 0.0001$), whereas no significant differences were detected among the other groups.

To assess the impact of dietary regimens on glycaemic regulation over time, serum glucose levels were measured at 0, 4, 8 and 12 weeks.

In Figure 4A, within-group comparisons revealed distinct temporal trajectories. In control animals (CT), serum glucose levels increased significantly between week 0 and week 8 ($p < 0.05$), and further between week 0 and week 12 ($p < 0.05$). In the FRUC group, a transient rise in serum glucose was observed at week 4, exceeding 400 mg/dL compared with baseline ($p < 0.05$), but no further changes were detected at later time points. The HFD group exhibited a significant increase in serum glucose between week 0 and week 8 ($p < 0.01$), reaching a value exceeding 400 mg/dL. In contrast, the combined HFD + FRUC group showed sustained hyperglycaemia, with significant elevations at both week 8 ($p < 0.01$) and week 12 ($p < 0.05$) exceeding 500 mg/dL relative to baseline.

In Figure 4B, between-group comparisons revealed no significant differences at week 0. At week 4, the FRUC group displayed significantly higher glucose levels than the CT group ($p < 0.01$), suggesting an early glycaemic perturbation induced by fructose alone. By week 8, only the HFD + FRUC group showed significantly elevated glucose compared to CT ($p < 0.05$). While no statistically significant intergroup differences were detected at week 12, glycaemic

profiles appeared to converge across groups. Notably, the comparison between CT and HFD + FRUC approached significance (p = 0.0672), suggesting a potential trend toward late-stage divergence.

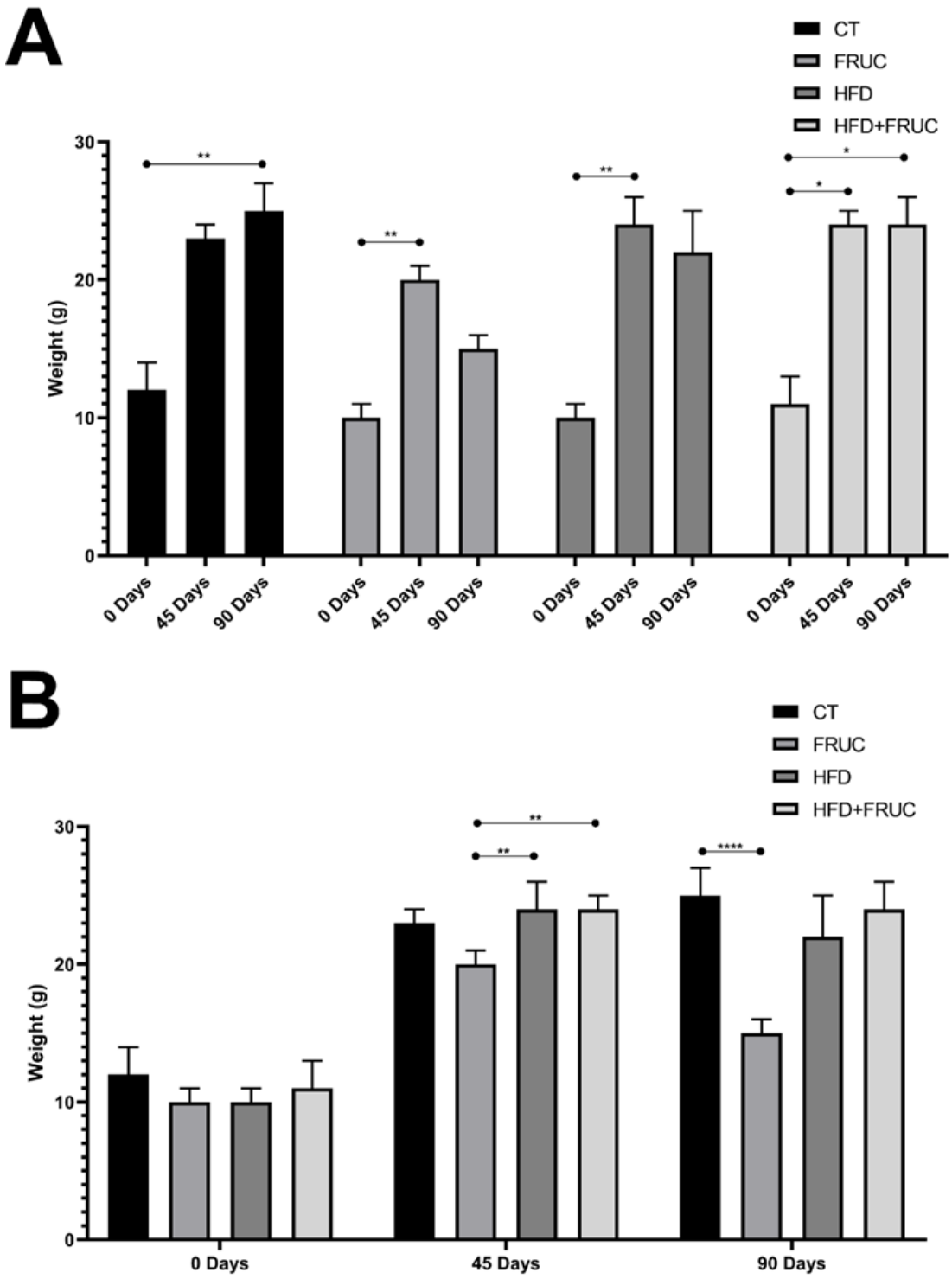

Figure 3.

Weight changes observed during the standardisation of the diabetes murine model

The graphs represent the weight gain in four groups of mice fed with standard diet (CT, n = 5), a standard diet supplemented with fructose (FRUC, n = 5), a high-fat diet (HFD, n = 5), or a high-fat diet supplemented with fructose (HFD + FRUC, n = 5) over a period of 0, 45 and 90 days. Panel A shows weight gain comparisons at each time point within each diet group, while panel B compares weight gain across the different diet groups at the specified time points. Significant weight increases were observed between the HFD and HFD + FRUC groups compared to the FRUC group on day 45, but at day 90, there was a significant decrease in weight between the FRUC and CT groups. Statistical significance is indicated as $p < 0.05$ (*), $p < 0.01$ (**) and $p < 0.0001$ (****).

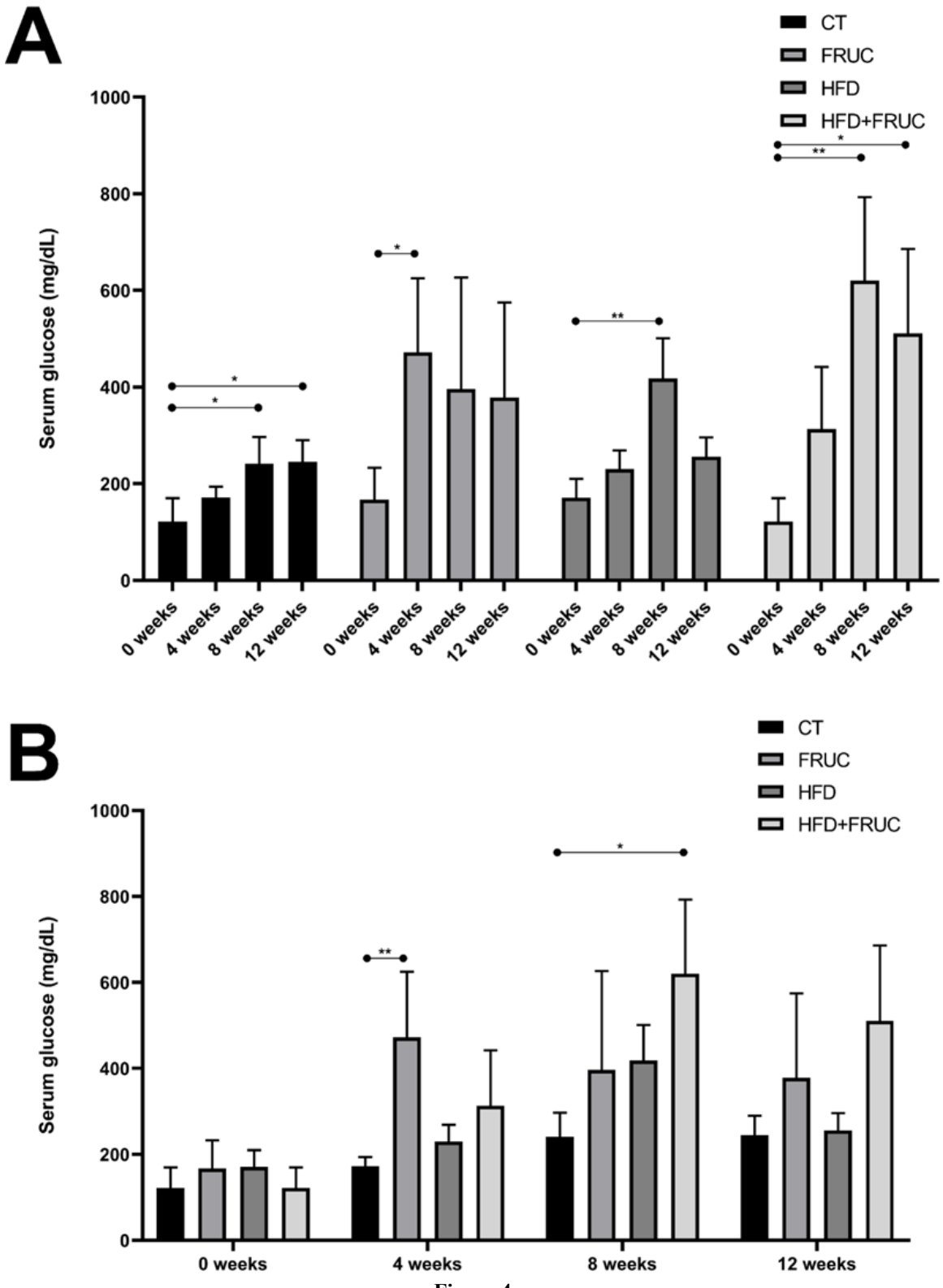

Figure 4.

Serum glucose changes observed during the standardisation of the diabetes murine model

The graphs depict serum glucose levels in four groups of mice fed with a standard diet (CT, n = 5), a standard diet supplemented with fructose (FRUC, n = 5), a high-fat diet (HFD, n = 5), or a high-fat diet supplemented with fructose (HFD + FRUC, n = 5) at 0, 4, 8 and 12 weeks. Panel A shows intra-group changes in glucose levels over time, while panel B compares glucose levels across the different diet groups at each time point. Significant increases in serum glucose were observed in the FRUC compared to CT in the 4th week. However, in week 8, HFD + FRUC was significantly higher compared to CT. Statistical significance is indicated as $p < 0.05$ (*), $p < 0.01$ (**), $p < 0.001$ (***) and $p < 0.0001$ (****).

It is noteworthy that in HFD + FRUC, the serum glucose was near 300 mg/dL by the 4th week, but after streptozocin administration, it increased, showing an almost 2-fold increase by the 8th week, and by the 12th week, this value was reduced by almost 15% compared to baseline. In the other groups, streptozocin administration did not appear to exert a considerable effect. For instance, in FRUC, streptozocin did not lead to a significant increase in glycemia. In mice fed an HFD, streptozocin administration led to a 2-fold increase in glycemia, but this change was not significant. Additionally, glycemia was almost restored by the 12th week, with a reduction of nearly 100%. For this reason, we chose the HFD + FRUC in combination with streptozocin as the best conditions to induce diabetes in the murine model.

Other groups have reported the development of glucose intolerance resembling T2DM in murine models after feeding with a high-fat diet supplemented with fructose and exposure to a low dose of streptozocin. Barriere *et al*. reported the induction of T2DM features in a murine model exposed to a high-fat, high-fructose diet for 56 weeks and to streptozocin (20 mg/kg) at weeks 2, 8, 14 and 20 [25]. On the other hand, Kim *et al*. reported the development of IR in a murine model fed with a high-fat diet and supplemented with fructose for 18 weeks and exposed to two doses of streptozocin (65 mg/kg) 4 weeks before euthanasia [26]. Additionally, Yin *et al.* reported the acquisition of hallmarks of T2DM in a murine model fed with a high-fat diet or a high-fat and sucrose diet and exposed to one (100 mg/kg) or two (50 mg/kg) doses of streptozocin in a single or consecutive days, respectively [27]. Our results partially agreed with the reports of Barriere *et al*. and Kim *et al*. because the best diet to induce features of T2DM in our model seems to be the combination of the high-fat diet and the supplementation with fructose, but not with the report of Yin *et al*. because the best condition was the high-fat diet with no supplementation with carbohydrates. For instance, according to Barriere *et al.*, by the 20th week, plasma glucose was near 10 mM after four administrations of streptozocin, whereas our murine model reached values of 22 - 33 mM by the 4 - 12 weeks, especially in the FRUC and HFD + FRUC regimens. Regarding weight, our murine model showed almost 2-fold increases in all groups, except in the FRUC group, at 6 - 12 weeks, while Barriere *et al*. reported modest increases in weight that tended to reach a 2-fold increase by 56 weeks. Comparing our results with those reported by Yin *et al*., they described increases in plasma glucose near 15 mM after the streptozocin administration in the high-fat diet group in the 5th week, but the mice that received both the high-fat diet and carbohydrate supplementation did not. This observation partially agrees with our results because in our study, the onset of the early hyperglycaemia appears to be primarily driven by fructose supplementation, whereas the contribution of HFD becomes more pronounced at later stages.

Modulation of hyperglycemia in the diabetic murine model treated with pioglitazone or recombinant PPARγ

Once the diabetic murine model was established, three groups of mice (each with n = 5) were diabetized employing the high-fat diet supplemented with fructose, and the exposure to streptozocin. One group of diabetized mice was treated with pioglitazone (DB + PIO), another with recombinant PPARγ (DB + PPARγ), while the last diabetized group remained untreated (DB). In the DB + PPARγ group, diabetic mice were treated with recombinant PPARγ to directly evaluate the effects of PPARγ activation, as the antidiabetic action of pioglitazone is primarily attributed to its interaction with this receptor. This approach enabled us to distinguish the molecular effects specifically mediated by PPARγ from those potentially resulting from PPARγ-independent mechanisms triggered by pioglitazone in the DB + PIO group. By comparing these groups, we aimed to identify additional molecular pathways or targets influenced by pioglitazone beyond its canonical activation of PPARγ. Notably, two mice from each group were excluded from the experiments based on exclusion criteria we established.

At baseline, in the 9th week, both groups displayed severe hyperglycaemia, with mean glucose levels exceeding 400 mg/dL. After diabetes induction, DB + PIO or DB + PPARγ mice were treated with the pioglitazone or recombinant PPARγ, respectively, in the 11th week (day 81), and glycemia was monitored 48 hours later to confirm the pharmacological effect in our murine model. As shown in Figure 5, the serum glucose concentration was significantly lowered either in the DB + PIO or DB + PPARγ groups in almost half (PPARγ: $p < 0.05$; PIO: $p < 0.0001$). In the 12th week (day 88), the mice received another dose of pioglitazone or recombinant PPARγ, and, as expected, glycemia was not significantly different from that obtained in the 11th week (PPARγ: $p < 0.01$; PIO: $p < 0.0001$).

Interestingly, a statistically significant difference was observed between the two treatments at baseline, with the PIO group exhibiting higher glycaemia compared to the PPARγ group ($p < 0.05$). However, no significant differences were detected between groups at later time points, suggesting that both interventions ultimately achieved comparable glycaemic control by day 88.

Modulation of triglycerides in the diabetic murine model treated with pioglitazone or recombinant PPARγ

As PPARγ activation influences the metabolism of both carbohydrates and lipids, we decided to evaluate the impact of pioglitazone or PPARγ treatment on serum triglycerides in the established diabetic murine model. As shown in Figure 6, serum triglyceride concentrations were significantly lower in the treated groups (DB + PPARγ or DB + PIO) than in the diabetic group.

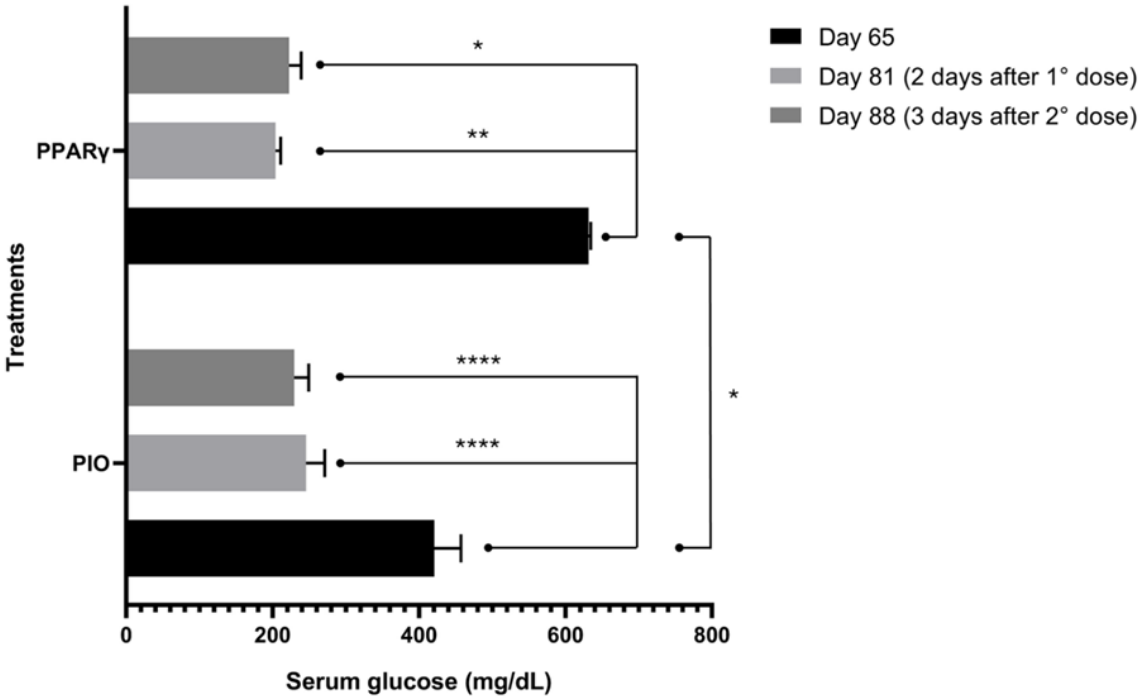

Figure 5.

Glycemia in the murine diabetes models DB + PIO and DB + PPARγ after treatment with pioglitazone and recombinant PPARγ, respectively

The graph shows serum glucose levels in diabetic mice induced with HFD + FRUC and treated with either pioglitazone (DB + PIO, n = 3) or recombinant PPARγ (DB + PPARγ, n = 3). Both treatments significantly reduced serum glucose levels compared to baseline. Statistical significance is indicated as $p < 0.05$ (*), $p < 0.01$ (**), $p < 0.0001$ (****).

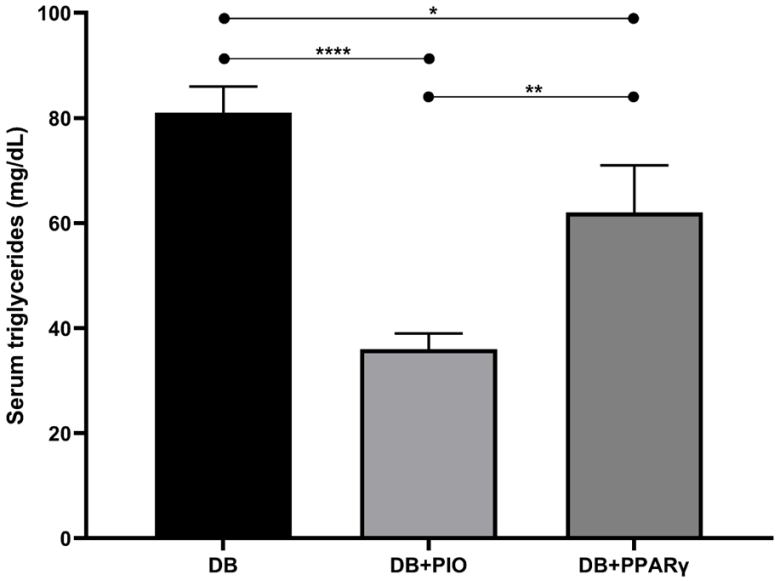

Figure 6.

Serum triglyceride concentration in diabetic murine models DB, DB + PPARγ and DB + PIO

The bar graph illustrates serum triglyceride concentrations in diabetic mice fed a high-fat diet supplemented with fructose (DB, n = 3), treated with either recombinant PPARγ (DB + PPARγ, n = 3) or pioglitazone (DB + PIO, n = 3). Treatment with pioglitazone (DB + PIO) or recombinant PPARγ significantly reduced serum triglyceride levels compared to the untreated diabetic group (DB). Statistical significance is indicated as $p < 0.05$ (*), $p < 0.01$ (**) and $p < 0.0001$ (****).

Contrary to our previous results, triglycerides were more strongly affected by pioglitazone in the DB + PIO group, with a significant reduction of approximately 50% in triglyceride concentration. In the case of DB + PPARγ, the observed mild reduction was near 20%. Notably, pioglitazone treatment significantly

reduced serum glucose and triglyceride levels, consistent with its known effects on glucose and lipid metabolism. Interestingly, pioglitazone exerted broader molecular effects than recombinant PPARγ, modulating a wider range of genes and pathways. This suggests that pioglitazone may exert PPARγ-independent actions, possibly involving crosstalk with other signalling pathways.

Modulation of the liver tissue transcriptome in the diabetic murine model treated with PPARγ or pioglitazone

To assess the molecular actions of pioglitazone over the murine model of diabetes, the liver was extracted from the euthanised mice after completion of the drug regimen. The total RNA was extracted from liver cells, then retrotranscribed and labelled for transcriptomic analysis *via* microarray. Then, the labelled cDNAs from each group were added to the DNA chips to be hybridised and read. The transcriptomic analysis showed that the liver tissue of the DB + PIO group exhibited upregulation of 310 genes and downregulation of 400 genes compared with the DB group. On the other hand, the DB + PPARγ group showed up-regulation of 300 genes and downregulation of 332 genes compared with the DB group. When upregulated or downregulated genes from DB + PPARγ and DB + PIO were compared, we observed that 102 and 161 genes, respectively, were commonly altered in both conditions.

To begin our path to identifying new druggable pathways or targets for the treatment of T2DM, based on the molecular actions of PPARγ activation, we again compared the differentially expressed genes and the genes involved in T2DM or IR, collected from GeneCards, using Venn diagrams. This comparison showed 85 downregulated and 50 upregulated genes in response to pioglitazone treatment, which were concordant with T2DM genes from GeneCards. Compared with the IR genes in GeneCards, 151 genes were downregulated and 115 were upregulated by pioglitazone treatment. Comparing the IR genes from GeneCards with the differentially expressed genes induced by PPARγ treatment, 131 genes were down-regulated and 97 were upregulated. Finally, compared with T2DM genes, we identified 77 downregulated and 38 upregulated common genes.

The up- or downregulated genes common to those associated with either T2DM or IR were functionally annotated using the ShinyGO 0.81 tool. In the KEGG database, our results showed that pioglitazone treatment induced statistically significant enrichment in pathways related to carbohydrate metabolism, the development of diabetic complications and hormonal signalling, among others. For instance, the pioglitazone-upregulated genes common to IR were involved in FoxO signalling, hypertrophic cardiomyopathy and PI3K-Akt signalling, among others. On the contrary, the downregulated genes commonly associated with AGE-RAGE signalling, hepatitis B and C and the signalling of relaxin and PI3K-Akt, among others. In the case of pioglitazone-upregulated genes common to T2DM, these were enriched in pathways such as FoxO signalling. In contrast, the downregulated genes were involved in AGE-RAGE signalling, hepatitis B and C and the PI3K-Akt signalling pathway, among others. A subset of the enriched pathways is shown in Table II, including the enriched genes and their enrichment scores.

Table II

Enriched pathways associated with IR or T2DM affected by pioglitazone or PPARγ

Enriched pathway	Enriched genes	E. Score
Upregulated genes affected by pioglitazone common to IR		
FoxO signalling pathway	*C8orf44-SGK3, EP300, SGK3, IL6, SGK1, SETD7*	0.006801972
PI3K-Akt signalling pathway	*C8orf44-SGK3, EFNA1, SGK3, IL6, ITGB3, LAMA3, SGK1, IKBKG, MAGI1*	0.006801972
MAPK signalling pathway	*EFNA1, MAPK8IP3, MAPK7, PTPRR, RPS6KA3, CACNB3, CACNG1, IKBKG*	0.007855967
Hypertrophic cardiomyopathy	*IL6, ITGB3, CACNB3, CACNG1*	0.031169087
Toll-like receptor signalling pathway	*IL6, TLR3, IKBKG, CD80*	0.037230293
Downregulated genes affected by pioglitazone common to IR		
Relaxin signalling pathway	*JUN, NOS3, MAPK1, RAF1, RELA, RLN1, TGFB1*	0.001837842
AGE-RAGE signalling pathway	*CDK4, JUN, NOS3, MAPK1, RELA, TGFB1*	0.002244014
PI3K-Akt signalling pathway	*CDK4, COL6A1, IFNA7, IFNAR1, IGF1R, ITGB7, NOS3, MAPK1, RAF1, RELA*	0.002851668
FoxO signalling pathway	*IGF1R, PRKAG2, MAPK1, RAF1, TGFB1*	0.0127892
Lipid and atherosclerosis	*IFNA7, JUN, NCF2, NOS3, MAPK1, RELA*	0.01809594
Upregulated genes affected by pioglitazone common to T2DM		
FoxO signalling pathway	*EP300, IL6, SGK1, SETD7*	0.01663987
Thyroid hormone signalling pathway	*EP300, ITGB3, THRB, NCOR1*	0.01663987
Viral life cycle HIV-1	*EP300, MX1, FURIN*	0.018169213
Influenza A	*EP300, IL6, MX1, TLR3*	0.022778316
Human papillomavirus infection	*EP300, ATP6V0A2, ITGB3, MX1, TLR3*	0.027847161

Enriched pathway	Enriched genes	E. Score
Downregulated genes affected by pioglitazone common to T2DM		
AGE-RAGE signalling pathway	*CDK4, JUN, NOS3, MAPK1, RELA, TGFB1*	0.000263505
PI3K-Akt signalling pathway	*CDK4, COL6A1, IFNAR1, IGF1R, NOS3, MAPK1, RAF1, RELA*	0.00086036
Taurine and hypotaurine metabolism	*GAD2, GGT1*	0.006513595
FoxO signalling pathway	*IGF1R, MAPK1, RAF1, TGFB1*	0.00651359
Diabetic cardiomyopathy	*NDUFS3, NOS3, RELA, TGFB1*	0.019738893
Downregulated genes affected by PPARγ common to IR		
Taurine and hypotaurine metabolism	*FMO3, GAD2, GGT1*	0.006513212
Protein processing in the E.R.	*STUB1, EIF2S1, DERL2, MAPK9, DNAJC1, SYVN1*	0.015786856
Fructose and mannose metabolism	*GMPPA, KHK, PMM1*	0.022531112
Lipid and atherosclerosis	*EIF2S1, IFNA7, JUN, NOS3, MAPK9, TRAF6*	0.033924941
Type II diabetes mellitus	*PRKCE, MAPK9, ABCC8*	0.034266215
Downregulated genes affected by PPARγ common to T2DM		
Protein processing in the E.R.	*STUB1, EIF2S1, DERL2, MAPK9, SYVN1*	0.01753819
AGE-RAGE signalling pathway	*CDK4, JUN, NOS3, MAPK9*	0.01753819
Lipid and atherosclerosis	*EIF2S1, JUN, NOS3, MAPK9, TRAF6*	0.021191996
Taurine and hypotaurine metabolism	*GAD2, GGT1*	0.025947938
IR	*NOS3, PPP1R3C, MAPK9*	0.04985681

IR: Insulin resistance; T2DM: Type 2 Diabetes mellitus; E. Score: Enrichment Score

Consistent with this, treatment with recombinant PPARγ induced a statistically significant enrichment in pathways related to AGE-RAGE signalling, PI3K-Akt signalling, IR, hepatitis and relaxin signalling, among others (Table II). However, the PPARγ treatment downregulated genes associated with IR or T2DM, including fructose and mannose metabolism, taurine and hypotaurine metabolism, apelin signalling, cholesterol metabolism and protein processing in the ER. It is noteworthy that there was no significant enrichment with the upregulated genes affected by PPARγ that were common to T2DM or IR.

The downregulation of the AGE-RAGE signalling pathway by pioglitazone treatment aligns with its reported anti-inflammatory and antioxidant properties. The reduction of key components such as NF-κB, JNK and NOS likely contributes to the attenuation of oxidative stress and inflammation, processes implicated in diabetic complications like atherosclerosis [28]. Advanced glycation end-products (AGEs) arise from the non-enzymatic glycation of proteins in conditions of hyperglycaemia. Low levels of AGEs are considered safe, as evidenced by the glycation of haemoglobin (HbA1c) that occurs during normoglycemia. However, in uncontrolled T2DM, high levels of AGEs are generated, leading to activation of their specific receptor, RAGE. When activated, RAGE promotes NF-κB pathway activation and increases NADPH oxidase activity, leading to a highly inflammatory and oxidative microenvironment. This scenario is involved in the development of atherosclerosis by promoting the proliferation and migration of smooth muscle cells from blood vessels [29]. Indeed, Low Wang *et al*. suggested that the pathophysiological mechanisms involved in T2DM are the most essential exacerbators of atherogenesis [30]. Regarding the AGE-RAGE pathway and thiazolidinediones, Gao *et al*. and Di *et al.* reported that pioglitazone decreased RAGE mRNA and protein levels in vascular smooth muscle cells, both *in vitro* and *in vivo* [31, 32]. In addition, this effect was due to pioglitazone-dependent activation of PPARγ, as this activity was abolished by the PPARγ inhibitor GW9662. Our results did not agree well with the previously reported effects on RAGE expression. Given that our findings do not align with those reported by Gao *et al*. and Di *et al*., it is essential to explore the AGE-RAGE pathway further experimentally. This could provide a deeper understanding of the underlying mechanisms and clarify the discrepancies observed, potentially offering new insights into the modulation of this pathway by pioglitazone in T2DM and related complications.

Additionally, pioglitazone downregulated the FoxO signalling pathway by increasing regulators such as SGK (coding for *SGK1*), SET7 (coding for *SETD7*) and p300 (coding for *EP300*), which inhibit FoxO activity. The FoxO proteins are transcription factors involved in the regulation of cell cycle, oxidative stress and the metabolism of carbohydrates, lipids and proteins, among other processes. There are four isoforms of this protein, including FoxO1, FoxO3, FoxO4 and FoxO6 [33]. However, FoxO1 and FoxO3 are the most studied regarding their role in the pathogenesis of T2DM. When FoxO is activated, it promotes the expression of genes involved in gluconeogenesis, such as *G6PC* and *PEPCK*, which encode glucose-6-phosphatase and phosphoenolpyruvate carboxykinase, respectively, leading to increased plasma glucose concentrations [33]. This activation occurs only under conditions of fasting or insulin resistance. Given that FoxO isoforms are transcription factors, their activity dependents on their transport into the nucleus by translocation. Indeed, this process is regulated by various post-translational modifications, such as phosphorylation, acetylation and methylation. For instance, in an insulin-sensitive scenario, the insulin-

dependent activation of Akt suppresses FoxO *via* direct phosphorylation. Another essential modification is acetylation by the histone acetyltransferases CBP/p300, which suppresses its translocation to the nucleus, leading to reduced expression of its target genes [33]. Other, less well-known regulatory elements of the FoxO pathway are SGK and SET7. The first one is a kinase whose activity is increased by insulin, leading to the phosphorylation of many proteins, including FoxO, thereby impairing its transcriptional activity. On the other hand, SET7 is a histone-lysine N-methyltransferase that regulates FoxO by methylation, reducing its translocation to the nucleus. Consistent with our results, pioglitazone treatment has been shown to increase SGK expression in the kidneys and gastric mucosa. Artunc *et al*. reported that in the kidney, pioglitazone-dependent SGK expression promotes ENaC expression, leading to increased sodium reabsorption and consequent intravascular volume expansion [34]. This explanation accounts for the oedema observed during long-term treatment with pioglitazone. On the other hand, Rotte *et al*. demonstrated that, in gastric mucosa, pioglitazone promoted the secretion of protons by increasing the abundance of KCNQ1 and H^+/K^+-ATPase in an SGK-dependent fashion [35]. Notably, *SETD7* and *EP300* have never been reported as target genes whose expression increased with pioglitazone treatment, or at least we could not find any such report.

Interestingly, the treatment with recombinant PPARγ selectively influenced pathways related to carbohydrate metabolism, such as fructose and mannose metabolism, and ER stress response. The downregulation of ketohexokinase, a key enzyme in fructose metabolism, highlights its potential as a novel therapeutic target for T2DM, particularly given the role of high fructose intake in IR and hyperlipidaemia. Ketohexokinase catalyses the phosphorylation of D-fructose in carbon 1, generating D-fructose-1-phosphate. This step represents D-fructose's commitment to carbohydrate metabolism. It is noteworthy that increased consumption of D-fructose has been linked to IR, obesity and hyperlipidaemia, among other conditions, yet D-fructose is a significant component of ultra-processed foods [36]. For this reason, ketohexokinase may be a good pharmacological target because its inhibition may result in a lower incorporation of D-fructose into metabolism, preventing the development of hyperinsulinemia or hyperlipidaemia, as reported by Gutierrez *et al*. [37]. Although there are some reports developing this idea, it has not been fully explored.

Additionally, attenuation of ER stress by recombinant PPARγ underscores its role in promoting cellular homeostasis and reducing apoptosis in diabetic conditions. The ER stress response is a process characterised by the appearance of high levels of misfolded proteins because of high rates of protein synthesis. This situation induces high expression of chaperones and components of the ubiquitin-proteasome system to promote the correct folding of these proteins, or their destruction if this is not accomplished. Our results showed downregulation of proteins involved in apoptosis induced by ER stress, such as JNK, or in the attenuation of protein synthesis, such as eIF2α. Indeed, Hong *et al.* reported that pioglitazone attenuate JNK activity and the expression of proinflammatory cytokines and markers of ER stress, such as p-eIF2α, in an *in vitro* model of pancreatic β-cells exposed to palmitate [38]. Additionally, these results were reproduced in the β-cell islets of an *in vivo* model. It is noteworthy that pioglitazone has been associated with the attenuation of ER stress *via* PPARγ activation in other models, including liver, macrophages and neural stem cells [39-41]. However, specific JNK inhibition was sufficient to increase cell viability and reduce markers of ER stress in an *in vitro* model of pancreatic cells exposed to IL-1β [42].

While our findings emphasise the therapeutic potential of pioglitazone, they also highlight the importance of distinguishing its PPARγ-dependent and independent actions. While both PIO and the recombinant PPARγ modulated overlapping pathways, PIO induced a broader range of gene expression changes, including the modulation of genes involved in FoxO signalling and PI3K-Akt signalling. In contrast, the treatment with recombinant PPARγ showed a more selective and limited modulation of pathways, particularly with significant enrichment in downregulated genes related to metabolic processes such as fructose and mannose metabolism, taurine and hypotaurine metabolism and apelin signalling. The lack of substantial enrichment in upregulated genes common to T2DM or IR suggests that recombinant PPARγ may not fully replicate the therapeutic effects of pioglitazone. This supports the hypothesis that actions of pioglitazone extend beyond direct PPARγ activation, potentially involving PPARγ-independent mechanisms or crosstalk with other signalling pathways. This distinction may pave the way for designing drugs that replicate the beneficial effects of pioglitazone while minimising its adverse outcomes. For example, targeting ketohexokinase or specific components of the AGE-RAGE or FoxO pathways may provide more selective and safer therapeutic strategies.

Despite these promising results, several limitations must be addressed. First, *in silico* predictions rely on existing databases and algorithms that may not fully capture the complexity of biological systems. Second, our experimental data were limited to liver tissue, excluding other critical organs such as adipose tissue and skeletal muscle, which play essential roles in glucose and lipid metabolism. Third, this study was designed with careful attention to ethical standards, including a deliberate effort to minimise animal use. While this approach reflects a strong commitment to the 3Rs principle (Replacement, Reduction, Refinement), it

may have inadvertently limited the statistical power of downstream analyses. Specifically, a separate cohort of animals was allocated for the experimental validation of the diabetes induction protocol, which, although helpful in confirming disease onset, reduced the number of animals available for randomisation into treatment groups. In retrospect, integrating all animals into a single randomised design guided by well-established models from the literature might have increased group sizes and improved statistical robustness without compromising scientific or ethical standards. Despite this limitation, the observed trends remained consistent and biologically meaningful, supporting the validity of the findings and underscoring the potential of the proposed interventions. Finally, future studies should include a multi-tissue approach and integrate other omics techniques, such as proteomics and metabolomics, to provide a more comprehensive understanding of the molecular actions of pioglitazone.

Conclusions

This study integrated *in silico* network pharmacology and experimental transcriptomics to elucidate the molecular mechanisms of pioglitazone in T2DM. Pioglitazone modulated key pathways, including PI3K-Akt, FoxO and AGE-RAGE signalling, validating computational predictions and revealing additional pathways, including carbohydrate metabolism and ER stress attenuation. Compared to recombinant PPARγ, pioglitazone exhibited broader molecular effects, highlighting PPARγ-independent mechanisms that contribute to its therapeutic potential. Novel targets, such as ketohexokinase and ER stress-related components, were identified, offering opportunities for developing more selective and safer T2DM treatments. Modulation of pioglitazone pathways involved in inflammation, oxidative stress and metabolic regulation reinforces its relevance in addressing diabetic complications. These findings provide a foundation for the next-generation therapies targeting specific molecular pathways while reducing adverse effects. The study emphasises the importance of combining computational and experimental approaches to advance drug discovery and improve therapeutic strategies for complex diseases like T2DM.

Conflict of interest

The authors declare no conflict of interest.

References

1. American Diabetes Association Professional Practice Committee, 2. Diagnosis and Classification of Diabetes: Standards of Care in Diabetes – 2024. *Diabetes Care*, 2024; 47(Supplement_1): S20-S42.
2. Aikaeli F, Njim T, Gissing S, Moyo F, Alam U, Mfinanga SG, Okebe J, Ramaiya K, Webb EL, Jaffar S, Garrib A, Prevalence of microvascular and macrovascular complications of diabetes in newly diagnosed type 2 diabetes in low-and-middle-income countries: A systematic review and meta-analysis. *PLOS Glob Public Health*, 2022; 2(6): e0000599.
3. Scărlătescu AI, Voicu SN, Pițuru MT, Apetroaei MM, Velescu BS, Udeanu DI, Nedea MI, Arsene AL, Probiotic effects on oxidative stress pathways in diabetes. *Farmacia*, 2024; 72(6): 1437-1449.
4. Grygiel-Górniak B, Peroxisome proliferator-activated receptors and their ligands: nutritional and clinical implications--a review. *Nutr J.*, 2014; 13: 1-10.
5. Hernandez-Quiles M, Broekema MF, Kalkhoven E, PPARgamma in Metabolism, Immunity, and Cancer: Unified and Diverse Mechanisms of Action. *Front Endocrinol (Lausanne)*, 2021; 12: 624112.
6. Rosen ED, Hsu CH, Wang X, Sakai S, Freeman MW, Gonzalez FJ, Spiegelman BM, C/EBPalpha induces adipogenesis through PPARgamma: a unified pathway. *Genes Dev.*, 2002; 16(1): 22-26.
7. Ohno H, Shinoda K, Spiegelman BM, Kajimura S, PPARγ agonists induce a white-to-brown fat conversion through stabilization of PRDM16 protein. *Cell Metab.*, 2012; 15(3): 395-404.
8. Quinn CE, Hamilton PK, Lockhart CJ, McVeigh GE, Thiazolidinediones: effects on insulin resistance and the cardiovascular system. *Br J Pharmacol.*, 2008; 153(4): 636-645.
9. Lebovitz HE, Thiazolidinediones: The forgotten diabetes medications. *Curr Diab Rep.*, 2019; 19(12): 151.
10. Kim HS, Hwang YC, Koo SH, Park KS, Lee MS, Kim KW, Lee MK, PPAR-γ activation increases insulin secretion through the up-regulation of the free fatty acid receptor GPR40 in pancreatic β-cells. *PLoS One*, 2013; 8(1): e50128.
11. Hevener AL, Olefsky JM, Reichart D, Nguyen MT, Bandyopadyhay G, Leung HY, Watt MJ, Benner C, Febbraio MA, Nguyen AK, Folian B, Subramaniam S, Gonzalez FJ, Glass CK, Ricote M, Macrophage PPAR gamma is required for normal skeletal muscle and hepatic insulin sensitivity and full antidiabetic effects of thiazolidinediones. *J Clin Invest.*, 2007; 117(6): 1658-1669.
12. Ahmadian M, Suh JM, Hah N, Liddle C, Atkins AR, Downes M, Evans RM, PPARγ signaling and metabolism: the good, the bad and the future. *Nat Med.*, 2013; 19(5): 557-566.
13. Viscoli CM, Inzucchi SE, Young LH, Insogna KL, Conwit R, Furie KL, Gorman M, Kelly MA, Lovejoy AM, Kernan WN; IRIS Trial Investigators, Pioglitazone and Risk for Bone Fracture: Safety Data From a Randomized Clinical Trial. *J Clin Endocrinol Metab.*, 2017; 102(3): 914-922.
14. Mori H, Okada Y, Tanaka Y, The Effects of Pioglitazone on Bone Formation and Resorption Markers in Type 2 Diabetes Mellitus. *Intern Med.*, 2017; 56(11): 1301-1306.
15. Miyazaki Y, Mahankali A, Matsuda M, Mahankali S, Hardies J, Cusi K, Mandarino LJ, DeFronzo RA, Effect of pioglitazone on abdominal fat distribution and insulin sensitivity in type 2 diabetic patients. *J Clin Endocrinol Metab.*, 2002; 87(6): 2784-2791.
16. Artunc F, Sandulache D, Nasir O, Boini KM, Friedrich B, Beier N, Dicks E, Pötzsch S, Klingel K, Amann K, Blazer-Yost BL, Scholz W, Risler T, Kuhl D, Lang

F, Lack of the serum and glucocorticoid-inducible kinase SGK1 attenuates the volume retention after treatment with the PPARgamma agonist pioglitazone. *Pflugers Arch.*, 2008; 456(2): 425-436.
17. DeFronzo RA, Tripathy D, Schwenke DC, Banerji M, Bray GA, Buchanan TA, Clement SC, Henry RR, Hodis HN, Kitabchi AE, Mack WJ, Mudaliar S, Ratner RE, Williams K, Stentz FB, Musi N, Reaven PD; ACT NOW Study, Pioglitazone for diabetes prevention in impaired glucose tolerance. *N Engl J Med.*, 2011; 364(12): 1104-1115.
18. Sheikh IM, Hassan OA, Adam SM, Ali AI, Ogedegbe OJ, Tabowei G, Barbarawi A, Yussuf FM, Nor MA, Association of Pioglitazone with Major Adverse Cardiovascular Events, All-Cause Mortality, and Heart Failure Hospitalizations: A Systematic Review. *Cureus.*, 2023; 15(10): e46911.
19. American Diabetes Association Professional Practice Committee, Summary of Revisions: Standards of Care in Diabetes-2024. *Diabetes Care*, 2024; 47(Suppl._1): S5-S10.
20. Daina A, Michielin O, Zoete V, SwissTargetPrediction: updated data and new features for efficient prediction of protein targets of small molecules. *Nucleic Acids Res.*, 2019; 47(W1): W357-W364.
21. Stelzer G, Rosen N, Plaschkes I, Zimmerman S, Twik M, Fishilevich S, Stein TI, Nudel R, Lieder I, Mazor Y, Kaplan S, Dahary D, Warshawsky D, Guan-Golan Y, Kohn A, Rappaport N, Safran M, Lancet D, The GeneCards Suite: From Gene Data Mining to Disease Genome Sequence Analyses. *Curr Protoc Bioinformatics*, 2016; 54(1): 1-30.
22. Shannon P, Markiel A, Ozier O, Baliga NS, Wang JT, Ramage D, Amin N, Schwikowski B, Ideker T, Cytoscape: a software environment for integrated models of biomolecular interaction networks. *Genome Res.*, 2003; 13(11): 2498-2504.
23. Ge SX, Jung D, Yao R, ShinyGO: a graphical gene-set enrichment tool for animals and plants. *Bioinformatics*, 2020; 36(8): 2628-2629.
24. Balderas-Renteria D, Montero-Molina S, Solis-Estrada J, Almaguer-Cantú V, Arévalo-Niño K, Zarate-Kalfópulos X, Balderas-Renteria I. Molecular cloning, expression, and purification of recombinant human PPARγ in *Escherichia coli*. *Revista BioTecnología*, 2023; 27(3): 28-39.
25. Barrière DA, Noll C, Roussy G, Lizotte F, Kessai A, Kirby K, Belleville K, Beaudet N, Longpré JM, Carpentier AC, Geraldes P, Sarret P, Combination of high-fat/high-fructose diet and low-dose streptozotocin to model long-term type-2 diabetes complications. *Sci Rep.*, 2018; 8(1): 424.
26. Kim Y, Stol M, Hebich B, Weng SY, Wang X, Shuppan D, Mice on a high-fat, high-fructose diet and treated with low dose streptozotocin develop features of human NASH. *Z Gastroenterol.*, 2012; 50(08): K036.
27. Yin R, Xue Y, Hu J, Hu X, Shen Q, The effects of diet and streptozotocin on metabolism and gut microbiota in a type 2 diabetes mellitus mouse model. *Food Agric Immunol.*, 2020; 31(1): 723-739.
28. Ramasamy R, Yan SF, Schmidt AM, Receptor for AGE (RAGE): signaling mechanisms in the pathogenesis of diabetes and its complications. *Ann N Y Acad Sci.*, 2011; 1243(1): 88-102.
29. Yuan G, Si G, Hou Q, Li Z, Xu K, Wang Y, Wang W, Xu X, Zhang L, Sun X, He H, Zeng H, Liu Y, Advanced Glycation End Products Induce Proliferation and Migration of Human Aortic Smooth Muscle Cells through PI3K/AKT Pathway. *Biomed Res Int.*, 2020; 2020(1): 8607418.
30. Low Wang CC, Hess CN, Hiatt WR, Goldfine AB, Clinical Update: Cardiovascular Disease in Diabetes Mellitus: Atherosclerotic Cardiovascular Disease and Heart Failure in Type 2 Diabetes Mellitus - Mechanisms, Management, and Clinical Considerations. *Circulation*, 2016; 133(24): 2459-2502.
31. Di BB, Li HW, Li WP, Shen XH, Sun ZJ, Wu X, Pioglitazone inhibits high glucose-induced expression of receptor for advanced glycation end products in coronary artery smooth muscle cells. *Mol Med Rep.*, 2015; 11(4): 2601-2607.
32. Gao H, Li H, Li W, Shen X, Di B, Pioglitazone Attenuates Atherosclerosis in Diabetic Mice by Inhibition of Receptor for Advanced Glycation End-Product (RAGE) Signaling. *Med Sci Monit.*, 2017; 23: 6121-6131.
33. Teaney NA, Cyr NE, FoxO1 as a tissue-specific therapeutic target for type 2 diabetes. *Front Endocrinol (Lausanne)*, 2023; 14: 1286838.
34. Artunc F, Sandulache D, Nasir O, Boini KM, Friedrich B, Beier N, Dicks E, Pötzsch S, Klingel K, Amann K, Blazer-Yost BL, Scholz W, Risler T, Kuhl D, Lang F, Lack of the serum and glucocorticoid-inducible kinase SGK1 attenuates the volume retention after treatment with the PPARgamma agonist pioglitazone. *Pflugers Arch.*, 2008; 456(2): 425-436.
35. Rotte A, Mack AF, Bhandaru M, Kempe DS, Beier N, Scholz W, Dicks E, Pötzsch S, Kuhl D, Lang F, Pioglitazone induced gastric acid secretion. *Cell Physiol Biochem.*, 2009; 24(3-4): 193-200.
36. Ter Horst KW, Schene MR, Holman R, Romijn JA, Serlie MJ, Effect of fructose consumption on insulin sensitivity in nondiabetic subjects: a systematic review and meta-analysis of diet-intervention trials. *Am J Clin Nutr.*, 2016; 104(6): 1562-1576.
37. Gutierrez JA, Liu W, Perez S, Xing G, Sonnenberg G, Kou K, Blatnik M, Allen R, Weng Y, Vera NB, Chidsey K, Bergman A, Somayaji V, Crowley C, Clasquin MF, Nigam A, Fulham MA, Erion DM, Ross TT, Esler WP, Magee TV, Pfefferkorn JA, Bence KK, Birnbaum MJ, Tesz GJ, Pharmacologic inhibition of ketohexokinase prevents fructose-induced metabolic dysfunction. *Mol Metab.*, 2021; 48: 101196.
38. Hong SW, Lee J, Cho JH, Kwon H, Park SE, Rhee EJ, Park CY, Oh KW, Park SW, Lee WY, Pioglitazone Attenuates Palmitate-Induced Inflammation and Endoplasmic Reticulum Stress in Pancreatic β-Cells. *Endocrinol Metab (Seoul)*, 2018; 33(1): 105-113.
39. Yoshiuchi K, Kaneto H, Matsuoka TA, Kasami R, Kohno K, Iwawaki T, Nakatani Y, Yamasaki Y, Shimomura I, Matsuhisa M, Pioglitazone reduces ER stress in the liver: direct monitoring of *in vivo* ER stress using ER stress-activated indicator transgenic mice. *Endocr J.*, 2009; 56(9): 1103-1111.
40. Ikeda J, Ichiki T, Takahara Y, Kojima H, Sankoda C, Kitamoto S, Tokunou T, Sunagawa K, PPARγ

Agonists Attenuate Palmitate-Induced ER Stress through Up-Regulation of SCD-1 in Macrophages. *PLoS One*, 2015; 10(6): e0128546.

41. Lin CH, Nicol CJB, Cheng YC, Chen SJ, Yen CH, Huang RN, Chiang MC, Rosiglitazone rescues human neural stem cells from amyloid-beta induced ER stress *via* PPARγ dependent signaling. *Exp Cell Res.*, 2018; 370(2): 312-321.
42. Verma G, Datta M, IL-1β induces ER stress in a JNK dependent manner that determines cell death in human pancreatic epithelial MIA PaCa-2 cells. *Apoptosis*, 2010; 15: 864-876.